

## **Carburization and Metal Dusting in Fired Heaters and Steam Methane Reformers: Plant Integrity Issues**

A. R. Franks, S. L. Bagnall

R-Tech Consultants Ltd, Testing House, Kenfig Industrial Estate, Margam, Port Talbot, SA13 2PE, UK

J. M. Brear, J. Williamson

John Brear – Plant Integrity, Abergefryn, Capel Seion, Drefach, Llanelli, SA147BP, UK

P. Conlin<sup>+</sup>, G. Reid<sup>#</sup>

Sonomatic Ltd, Dornoch House, The Links, Birchwood, Warrington, WA3 7PB, UK<sup>+</sup>

Sonomatic Ltd, c/o Emdad, Level 29, Etihad Office Tower 3, Al Ras Al Akhdar, Abu Dhabi<sup>#</sup>

### **ABSTRACT**

Safe and secure operation of critical plant items requires a recognition and an understanding of the processes that affect component integrity and life. Carburization is common in many fired heater tubes in hydrocarbon service; certain components in fluidized catalytic cracking units (FCCUs) can be affected and the issue is also known in steam methane reformers (SMRs). Though carburization is to be expected in such situations, it is not addressed by standard design and assessment procedures.

Carburization may interact with creep and with other wastage processes, leading to significant changes in rupture life; it may cause brittle failures leading to complete fracture and has been known to cause tube melting. It may also progress to metal dusting, leading to rapid loss of material.

This paper begins by describing these different phenomena and explains how they and their effects may be predicted. A non-destructive inspection technique for determining carburization depth, using a time of flight diffraction (TOFD) method, is presented and its integration into a predictive component life assessment methodology is described. Examples of recent assessments are given, showing the opportunities for life extension, process optimization and failure avoidance.

Key words: carburization, metal dusting, fired heater, steam methane reformer, life assessment, TOFD

### **THE CHEMISTRY OF CARBURIZATION AND METAL DUSTING**

Carburization and metal dusting are corrosion phenomena caused by the transfer of carbon from a hydrocarbon or other carbonaceous gas into the matrix of a metal – usually a steel or nickel-based alloy. Depending on its chemical activity, the carbon may be held in solution, it may form metal carbides, or it may be deposited internally in elemental form.<sup>1</sup> In every case, the physical and mechanical properties of the metal are affected in ways that potentially impact on plant integrity.

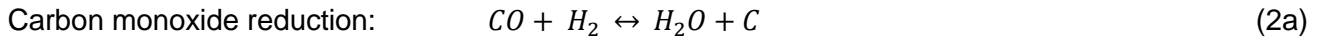
In a simple hydrocarbon environment, as present in refinery fired heaters and similar equipment (including certain FCCU components) the carbon is transferred by reactions of the type:



for which the carbon activity,  $a_c$ , is given by:

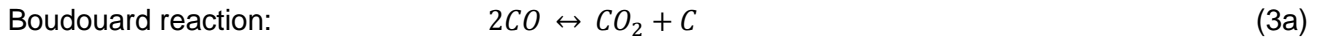
$$a_c = \left( \frac{K_H [C_m H_n]}{[H_2]^{\frac{n}{2}}} \right)^{\frac{1}{m}} \quad (1b)$$

where  $[.]$  denotes partial pressure and  $K_H$  is a species dependent equilibrium constant. For the more complex environments that pertain in steam methane reformers, two reactions are of interest:



for which:  $a_c = \left( \frac{K_C [CO] [H_2]}{[H_2O]} \right) \quad (2b)$

with:<sup>2</sup>  $\log(K_C) = \frac{7100}{T} - 7.496 \quad (2c)$



for which:  $a_c = \left( \frac{K_B [CO]^2}{[CO_2]} \right) \quad (3b)$

with:<sup>2</sup>  $\log(K_B) = \frac{8817}{T} - 9.071 \quad (3c)$

In the above temperature,  $T$ , is in Kelvin and  $K_H$ ,  $K_C$ ,  $K_B$  are dimensionless after allowance for the implied activity coefficients.

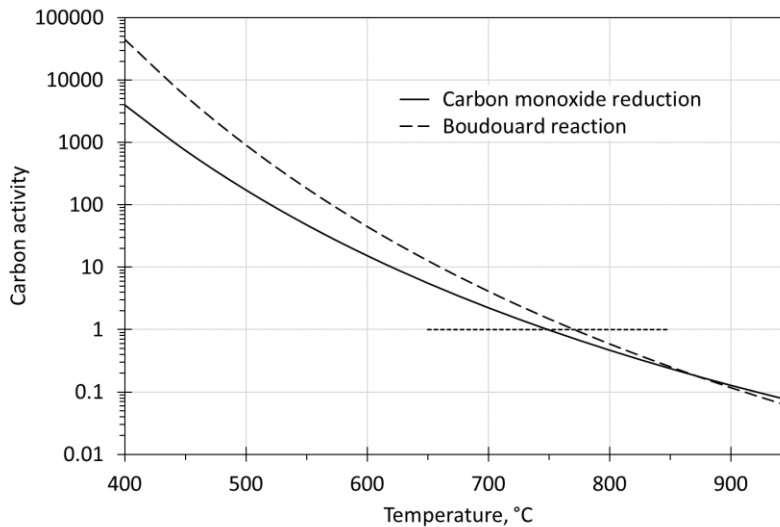


**Figure 1: Relation between carbon activity and temperature for a steam methane reformer**

A practical illustration of Equations 2, 3 is given in Figure 1. This pertains to a specific SMR with partial pressures at the catalyst tube outlet of:  $[CO] = 3.5$ ,  $[CO_2] = 2.9$ ,  $[H_2] = [H_2O] = 6.5$  bar. As will be discussed later, certain tubes in this reformer, which serves a combined refinery and petrochemical complex, are subject to carburization and metal dusting. The carbon activity reaches unity at around 775°C.

The above equations are generic to carburization reactions. The particular phenomenon of metal dusting arises when the carbon activity is greater than unity – i.e. when oversaturation occurs. It is manifest as graphite growth in or into the metal, leading to its disintegration into a fine dust comprising metal particles and carbon as graphite, in some cases also containing metal carbides and oxides.

### THE METALLURGY OF CARBURIZATION AND METAL DUSTING

The detailed metallurgy of carburization and metal dusting is controlled largely by the carbon activity and by the role of protective oxide films, particularly in the higher chromium steels.

#### Carburization

At low carbon activities,  $10^{-3} < a_c < 10^{-2}$ , carbon transferred into the metal forms carbides of composition  $M_{23}C_6$ ; as the activity rises,  $M_7C_3$  is preferred and as it approaches unity,  $M_3C$  and particularly cementite,  $Fe_3C$ , becomes dominant.<sup>1,2,3</sup> At unit activity, graphite is stable. Thus the gradients in etching response and hardness (Figure 2) which reflect the diffusion profile, are accompanied by a gradient in carbide type.

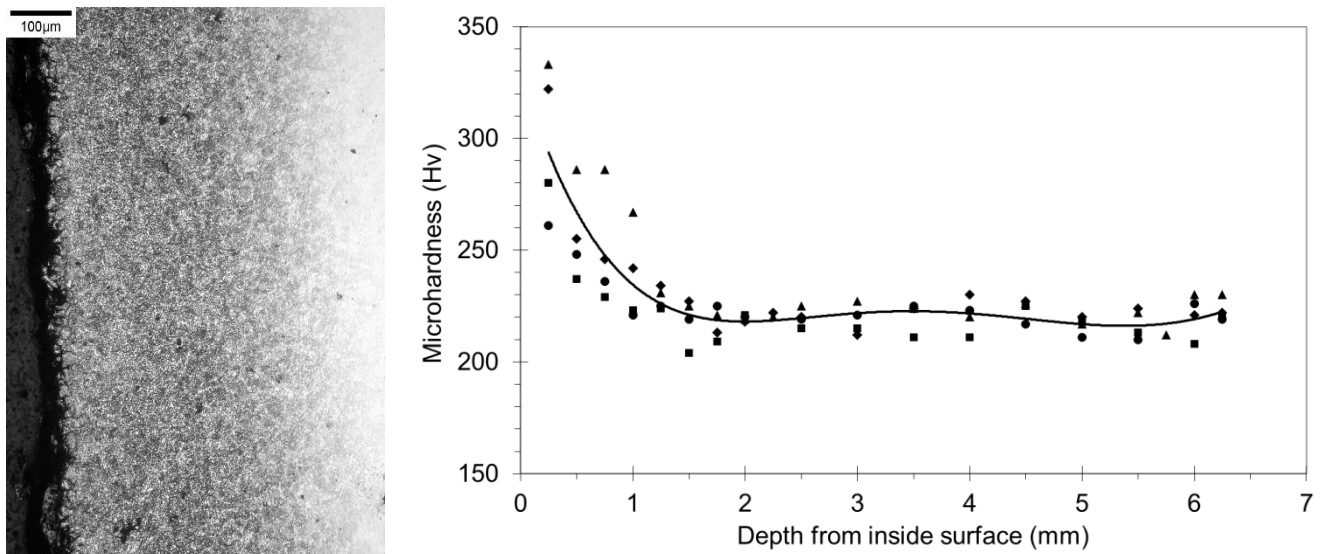
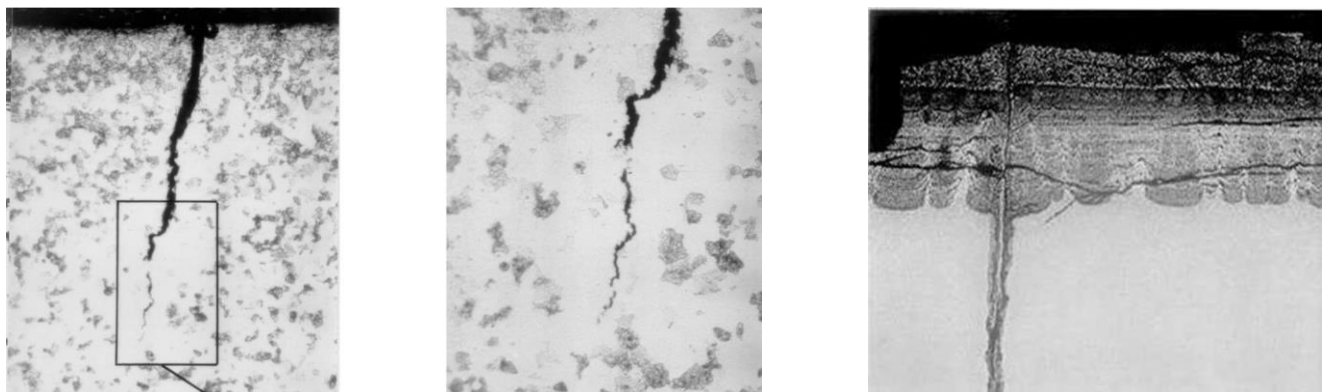


Figure 2: Etched section and hardness profile through the carburized layer in a 9CrMo tube



(a, b) progressive cracking of the carburized zone

(c) spalling

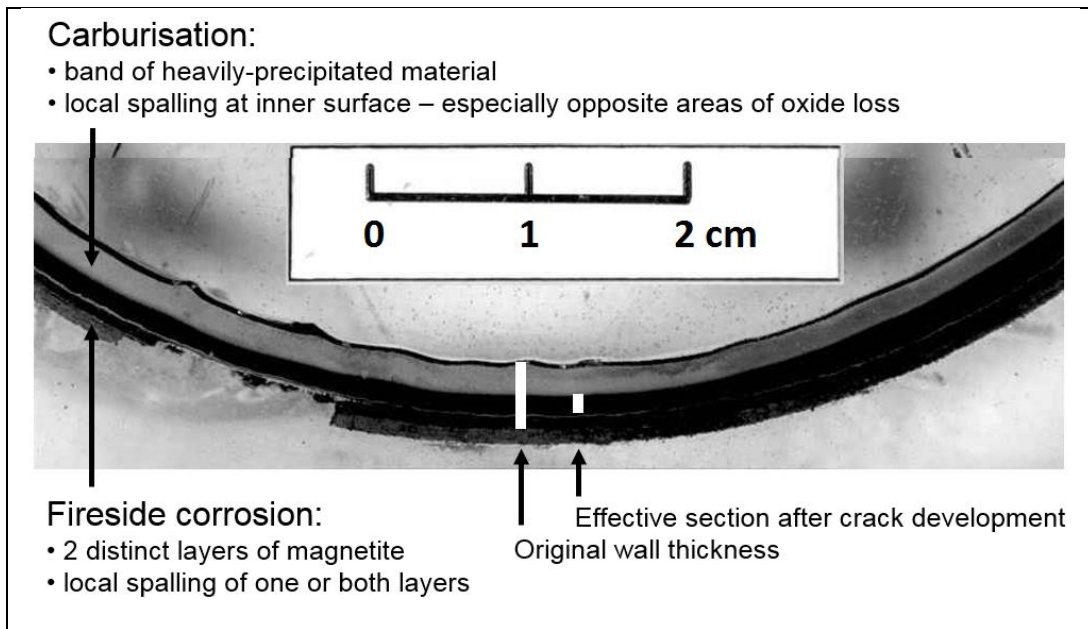
Figure 3: Crack development through the carburized layer in 9CrMo tubes

There is a volume expansion associated with carbon take-up, leading to local stresses, but at moderate carburization rates these redistribute, by creep, to low levels and the gross distortions seen in steam cracker tubes do not occur in fired heater or SMR tubes. As Grabke<sup>1</sup> points out, carburization leads to a deterioration in low temperature ductility and toughness, also to an increase in high temperature creep and tensile strength. However, the drop in high temperature ductility must not be underestimated. At moderate thicknesses the carburized layer can through-crack, most likely on plant shut-down due to stresses induced by the difference in thermal expansion between carburized and unaffected material (Figure 3a, crack depth ~ 1.5 mm). This cracking appears to progress step-wise (Figure 3b). Eventually spalling of the carburized layer occurs (Figure 3c, spalled thickness ~1 mm).

In simple hydrocarbon environments no protective oxide film develops to inhibit carbon transfer, but in gases containing significant steam or carbon dioxide such a passive film can form. Interactions between carburization and oxidation are discussed by Hansel et al.<sup>4</sup> In such circumstances, carburization cannot progress until the film is breached. Usually this break occurs mechanically – through creep or thermal strains – leading to local, rather than general, attack. At high carbon activities and high temperatures protection can be lost through conversion of chromium oxides to carbides,<sup>1</sup> leading to rapid attack.

### Interactions Between Carburization and Other Processes

The detrimental effects of carburization-induced cracking are obvious from the photographs shown in Figure 3. However, the initial strengthening effect of a carburized layer – so long as it remains intact – must not be forgotten. Comparative stress rupture tests on full wall thickness specimens from carburized tubes show that for 5CrMo and 9CrMo steels the creep life can be enhanced by a factor of three. Once the carburized zone begins to crack this strength advantage is lost; indeed, the zone can no longer be considered load-bearing. Both the strengthening and the effective loss of section effects must be considered in integrity assessments, and their interactions with other life-limiting processes must be accounted for.



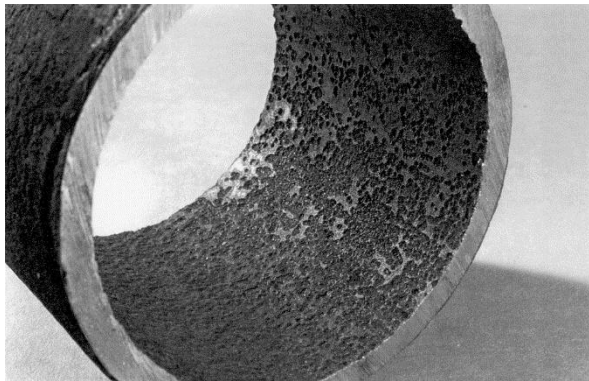
**Figure 4: Through-wall section of a 9CrMo CCR heater tube**

Figure 4 shows the relevant features of a 9CrMo continuous catalytic reformer (CCR) heater tube subject to fireside oxidation and internal carburization. The light-etching band, extending to around half the remaining tube wall thickness and corresponding to the carburized zone, is clear. At this magnification the cracking is not visible, but this tube is from the same heater as those shown in Figure 3 and cracks are present. Evidence of the associated spalling is visible. At the outer surface the double magnetite

layer produced by fireside corrosion is seen, the interface between the layers corresponding to the original metal surface. Local spalling of one or both layers is evident. The white bars denote the original wall thickness and the current effective load-bearing section. In combination, therefore, carburization and fireside corrosion can lead to losses in section and corresponding increases in stress that greatly accelerate creep life consumption.

### **Metal Dusting**

Metal dusting can manifest in several ways, as seen in Figure 5. Pitting, either widespread or local, is common as seen in the 5CrMo heater tube shown in Figure 5a.<sup>5</sup> Areas of enhanced heat flux provide preferential sites, as evidenced by the leak at the thermocouple installation on the 9CrMo CCR tube shown in Figure 5b (courtesy UOP). In certain instances a pit can develop preferentially, leading to penetration of the tube wall as seen in the 5CrMo crude heater tube shown in Figure 5c. The volume expansion associated with dust formation is seen to lead to a general out-of-roundness and a local extrusion of tube metal forward of the growing pit. The light-etching halo of carburized material surrounding the pit is also evident in this photograph. In the extreme, melting of the tube can occur, Figure 5d. This is associated with the fall in solidus temperature associated with high carbon levels and overheating effects where the 'dust' remains adherent to the tube wall.



(a) General pitting



(b) Local thinning at a hot-spot



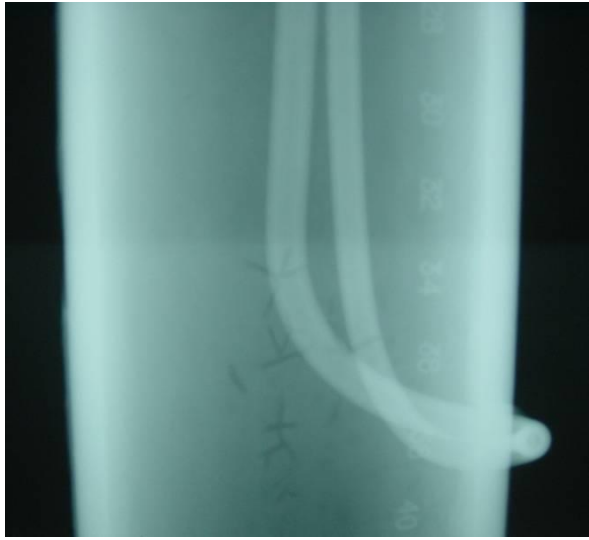
(c) Preferential development of a single pit



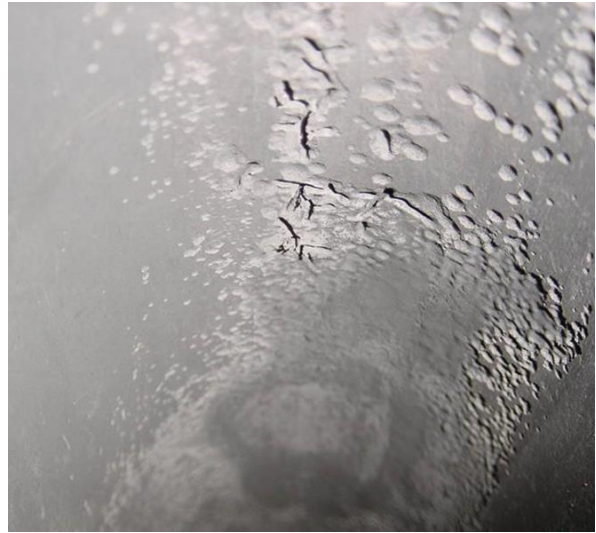
(d) Widespread melting

**Figure 5: Manifestations of metal dusting**

A further manifestation of metal dusting has been reported.<sup>6,7</sup> It was named 'crow's foot' cracking, by the refinery that first reported it, due to its morphology. Representative images, from 9CrMo tubes in CCR service, are shown in Figure 6.



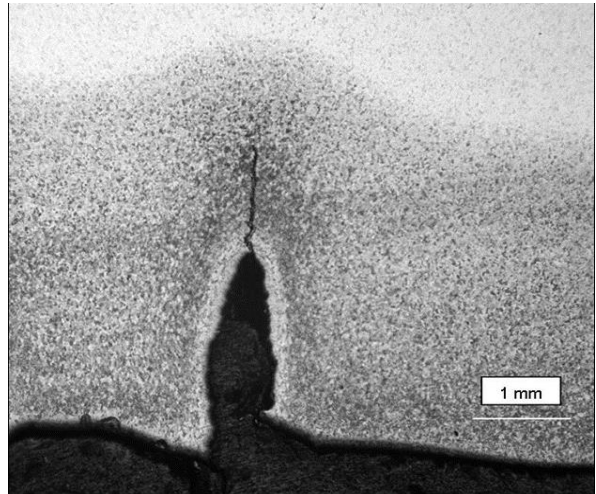
(a) Radiographic image



(b) Video-camera image



(c) Macro-photograph



(d) Metallographic section

### Figure 6: The 'Crow's foot' cracking phenomenon

Radiography, performed after a tube leak, revealed characteristic but unrecognized features, resembling a bird's footprints, (Figure 6a). A video-camera inspection showed that these were cracks with unusual raised edges, associated with the pitting typical of metal dusting (Figure 6b). The photograph of a sectioned tube (Figure 6c) shows the morphology more clearly. A metallographic section (Figure 6d) elucidates the mechanism. A general, and deep, carburized layer is apparent, with a wide crack extending to around half its depth. This crack was tightly packed with typical dust. The associated volume expansion had widened the crack and forced tube metal to the surface, creating the raised edges to the cracks. A narrow crack extends a further 1.5 mm into the material and, as it provides a rapid diffusion path for carbon, the carburized zone is seen to be further developed local to the crack than elsewhere. This progressive cracking resembles that seen in Figure 3 and suggests the following sequence of events, which was confirmed by retrospective re-examination of samples taken at a previous outage. For some time, the tubes operated under circumstances where carburization occurred, but not metal dusting. The normal increase in carburization depth and progressive cracking took place. Later, changes in operation, discussed below, rendered the tubes susceptible to metal dusting. At the surface this produced the usual pitting, seen in Figure 6b – but it also took place within the existing cracks, leading

to the crow's foot mode of development as the cracks filled with the metal dust and were forcibly widened. The random direction of the cracks reflects the bi-axiality of the thermal stresses that lead to their formation.

### THE NON-DESTRUCTIVE MEASUREMENT OF CARBURIZATION AND METAL DUSTING

As carburization and metal dusting take place at the inner surface of the subject types of tube, for many years the only method of ascertaining the presence and extent of these processes was by destructive sampling. This was expensive and disruptive, and opened the possibility that a sampled tube was found to be so severely carburized that weld repair was impossible.

As a result of the authors' work on the above CCR problems, there is now an established non-destructive inspection technique, based on ultrasonic time-of-flight-diffraction (TOFD),<sup>9</sup> which can measure the depth of carburization without the need to remove samples. The inspection protocol and set-up parameters are critical to the ability of this technique to locate and identify carburization damage, as it is possible to carry out a standard TOFD inspection and not identify any carburization present. Figure 7 shows examples of the work done by the authors to validate this technique. The graph compares measurements of carburized zone depth obtained by TOFD with those obtained by destructive metallography. It indicates a resolution limit at around 0.5mm and an excellent correlation above 1.5mm. The photographs show the TOFD scan (top) of an area containing both uniform carburization and a crow's foot crack (centre). Clear resolution of both phenomena is apparent and the accuracy of the depth measurements, crudely demonstrated by means of a ruler (bottom), was very high – the crow's foot crack contributing the highest point to the graph at the left.

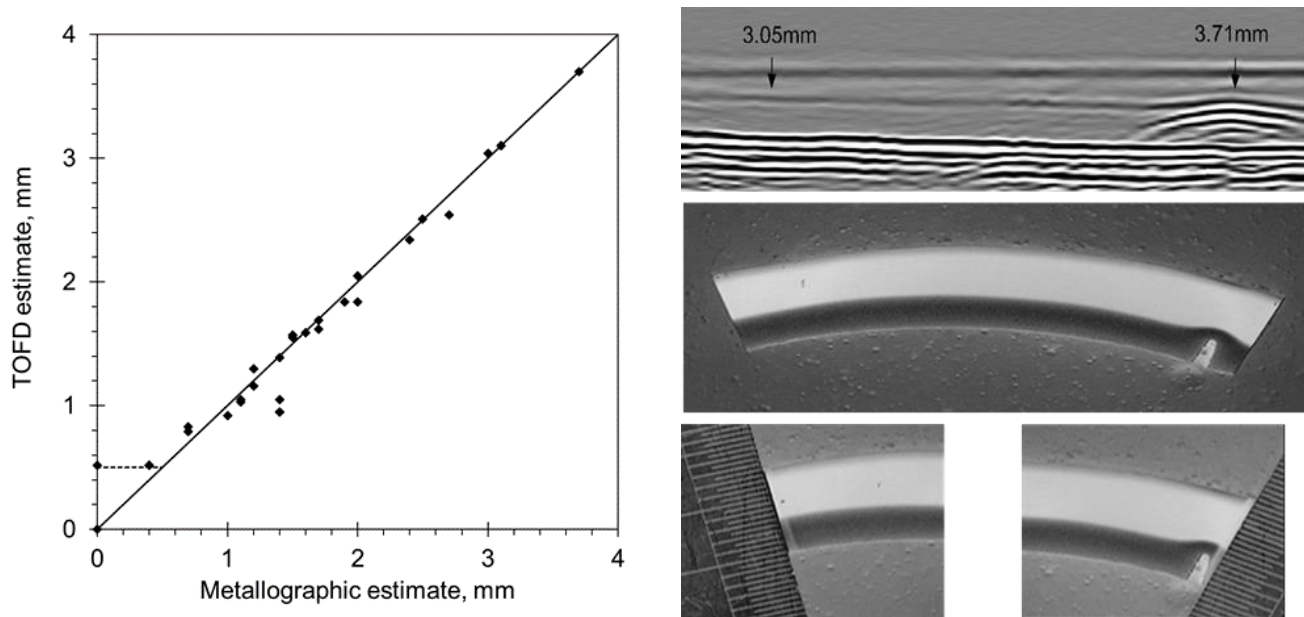


**Figure 7: Validation of the TOFD technique for carburization, left, and crow's feet, right**

Confidence in the technique for detecting and measuring carburization is high. Metal dusting, as its occurrence is often localized, can be more problematic to detect, but when detected, measurement accuracy is good. The technique also determines the tube wall thickness.

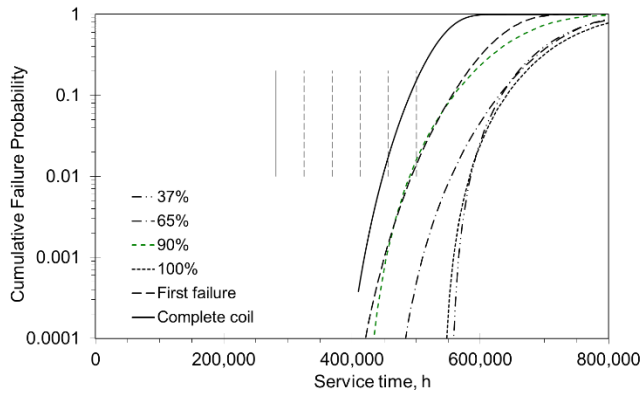
### REMAINING LIFE PREDICTION, ACCOUNTING FOR CARBURIZATION AND METAL DUSTING

Procedures such as API RP530<sup>8</sup> provide a simple but reasonable approach to the prediction of fired tube life under a combination of creep and fireside corrosion. However, as yet, no current industry-standard procedures allow for the effects of carburization. Development of such a procedure requires a model of

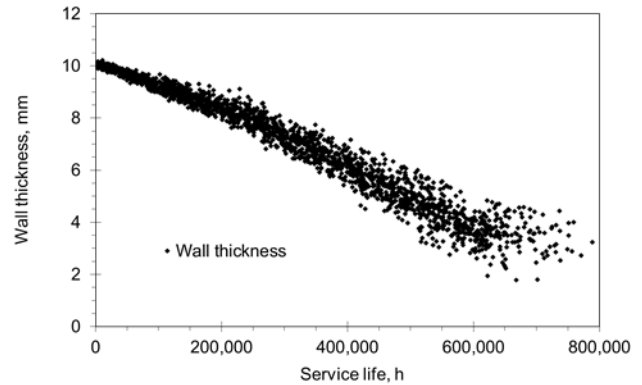
the combined creep-carburization-corrosion process and a means of measuring and predicting the progress of carburization.

The method adopted in API RP530 is to sum creep life fractions based on a partitioning of the stress-temperature history, then correct the result for progressive fireside corrosion by application of an equation that is effectively an integral solution which assumes that the metal loss rate is constant. Were carburization simply a further wastage process, then it could be included relatively simply. However, this would be overconservative as it would neglect the very real benefit of the initial strengthening effect.

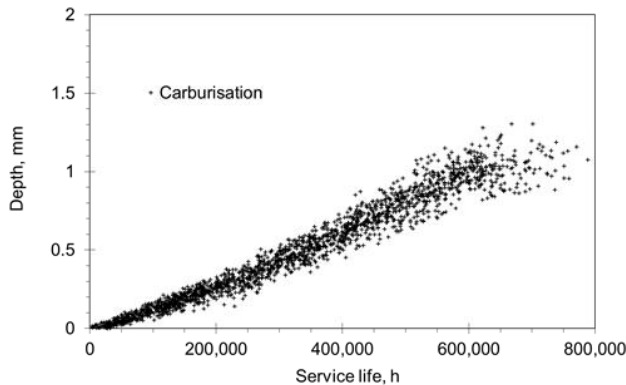
The integral solution approach has the advantage of computational simplicity, but is rather inflexible. Here, the alternative adopted is to use a differential method, based on the rate equations for creep, fireside corrosion and carburization. These are integrated forward in time to calculate the progressive increases in creep life consumption, metal loss, carburized zone depth and crack depth. Though computationally more intensive, this approach has the great advantage of total flexibility with regard to operational history – including such features as variation in conditions through run and the effects of major changes in operating regime. As it predicts evolution of component state in terms of parameters that are subject to comparison with inspection data, then the results can be validated and refined at each successive inspection outage. If set up using the same assumptions and input data, it generates identical results to those obtained following API RP530. Given the variations and uncertainties inherent in plant data, the model is embedded in a probabilistic shell so as to generate failure distributions rather than simple mean or lower-bound predictions.



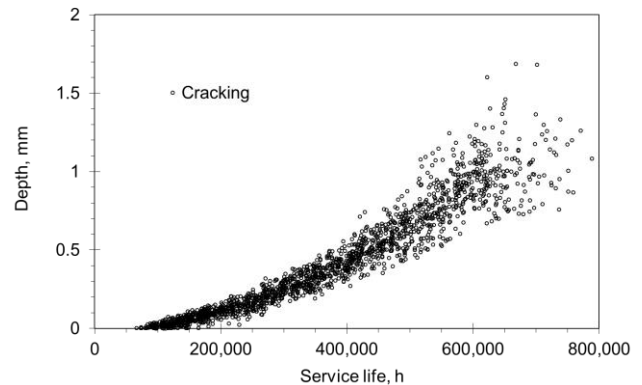
(a) Predicted failure probability



(b) Predicted fireside corrosion



(c) Predicted carburized zone thickness



(c) Predicted crack depth

**Figure 8: Probabilistic life prediction of a 9CrMo 48-pass coil in a visbreaker**

The example given in Figure 8 concerns a visbreaker. This cabin furnace contains two radiant cells, each with two almost-identical coils. A common convection section serves as process pre-heat to the radiant section and also contains a steam coil. Each radiant coil has 42 wall tubes and 6 roof tubes, all of 9Cr1Mo steel with 114.3 mm OD and 7.5 mm wall. There are four temperature measurement points on each coil, at 37, 65, 90 and 100% of length respectively. Representative samples of operating conditions were obtained, including process inlet and outlet temperatures and pressures, flow rates and thermal properties and tube metal (skin) temperatures. As is common in visbreakers, where an endothermic cracking reaction occurs, the tube skin temperature peaked at about 2/3 height of the furnace wall. Conventional ultrasonic thickness data obtained at past outages were used to establish the historic metal loss rates and the TOFD technique was used to measure carburization depths, at three axial positions on 18 selected tubes in each coil. Carburization depth was observed to rise steadily from Tube 1 to Tube 25 and thereafter remained steady. It was also seen to peak slightly at the mid-length of each tube.

The fireside corrosion and carburization rates derived from the inspection data were seen to be consistent with experience of this material in comparable service.

Figure 8 summarizes the results for the lead coil. Predicted failure probability curves are shown in Figure 8a. Curves are given for each tube where skin temperature data are available, designated by the position of the sensor along the total coil length. The shortest predicted life occurs at the 90% position, which fact immediately allows some focusing of future inspections. The longest predicted lives occur at the 37% and 100% (outlet) positions. A further curve shows the distribution of first-failure times, independent of position. Unsurprisingly in this case, it broadly follows the curve for the lead position, at 90% of coil length. While these results show the most critical positions in the furnace, and the lives associated with them, for planning purposes it is useful to integrate these probability curves over the complete tube set and obtain a failure probability curve for the coil as a whole. Comparing this curve with the vertical lines on the graph, which denote the present time and each of the planned 5-year operating campaigns, it is seen that operation for two further campaigns is well within the coil's capacity, but a third might be marginal. A re-run of the assessment at the next turnaround will clarify this.

Figures 8b, c, d show the predicted reduction in wall thickness and development of the carburized zone and associated cracking. Loss of section due to fireside corrosion is seen to be more significant than that due to cracking of the carburized zone. These graphs can be used as an immediate comparison against future inspection data. Any significant differences between prediction and observation will warrant investigation, as they will indicate either an error in the life prediction or some change in operational variables that needs to be accounted for.

In this instance, the operator was satisfied with the finding that at least two further operating regimes were possible. However, in some cases there are reasons to consider the possibility of other options. An example is provided by another, similar, visbreaker. This unit was only achieving a 20% breaking efficiency and consideration was being given to improving its economic benefit to the refinery. A feature of visbreaker operation is the tendency for coke deposition on the tube walls, particularly in the area where cracking of the feedstock occurs. A consequence is that the tube wall temperature rises, since the coke acts as an insulator. When the temperature reaches the defined safe operating limit (SOL) it becomes necessary to shut the unit down for decoking, an expensive inconvenience. Under the then current regime, the SOL was set at 620°C and the decoking interval was two years. Two possibilities suggested themselves, both requiring the SOL to be raised. One was to raise the overall operating temperature so as to improve the breaking efficiency. Initial process calculations indicated that that would bring the product stream out of limits in terms of asphaltene content. The other possibility was to keep the start-of-run condition the same, but to increase run length by allowing a higher SOL. Accordingly, the life prediction package was set to simulate a range of possible run length / SOL combinations and determine their effect on tube life. Figure 9 shows the results obtained. Predicted remaining life at the then current operating condition was over 290,000h. Increasing the SOL to 640°C allowed the decoke interval to be increased to three years whilst reducing the remaining life to a still-useful 160,000h. This was adjudged the optimum solution and was adopted.

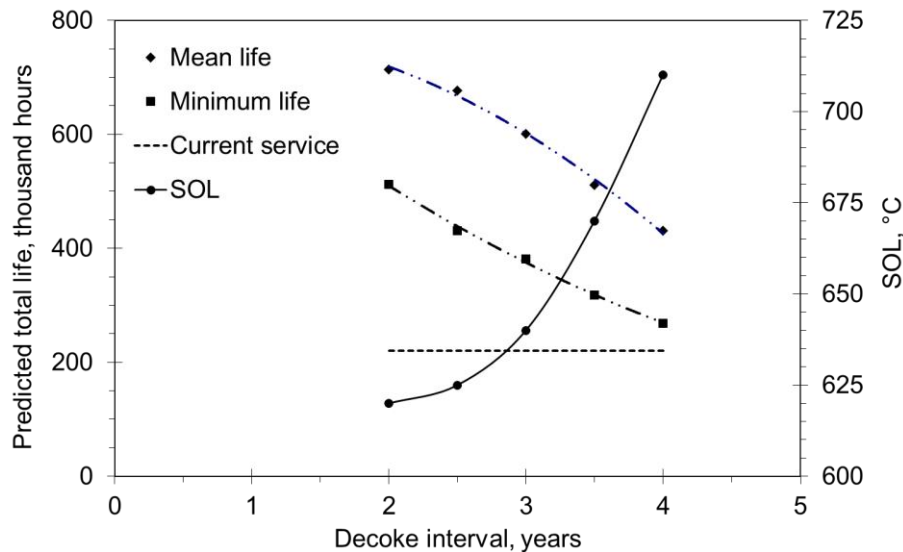


**Figure 9: Relationship between predicted life, decoke interval and SOL**

### FACTORS INFLUENCING CARBURIZATION AND METAL DUSTING

Carburization in refinery fired heaters tends to be specific to certain types of service – crude and vacuum heaters, coker heaters and visbreakers are often affected and share a trend in progressively increasing feedstock density. CCR heaters are also affected, not because their feed is heavy but because temperatures are high and by this stage in the process train the feed has often been purified of constituents that inhibit carbon transfer – particularly sulfur. **The CCR heater** which is the subject of Figure 6 moved from stable carburization to metal dusting following a significant increase (80degC) in process temperature and the addition of a fourth hydrofiner reactor immediately upstream. Installed to reduce nitrogen levels, **it also reduced sulfur below the 0.3ppm found by experience necessary to prevent metal dusting**. Reinjection of sulfur as dimethyl disulfide was found necessary to prevent the problem recurring.

In FCC units it has been found that partial combustion increases carburization of regenerator cyclones due to the increased CO/CO<sub>2</sub> ratio. The moves to allow riser cracking and to employ close coupling, both associated with short contact times, increase carburization and graphitization of reactor cyclones. Heavier feeds, particularly those with higher metal and sulfur levels, lead to increased carburization and graphitization of reactor cyclones and increased carburization and sigmatization of regenerator cyclones.

It is a widely-held belief that carburization and metal dusting are uncommon in SMR catalyst tubes – other than in very specific cases. There is increasing evidence that that is mistaken. At one time, catalyst tube life dominated SMR maintenance / life management. Improvements in tube metallurgy have changed the balance and the life of pigtails and other outlet system components is becoming an issue of importance. More examples of carburization and metal dusting are being seen, mainly at tube outlets, and it is arguable not that the phenomena are becoming more common but that achieved tube lives are such that they progress enough to become apparent.

This example concerns the SMR mentioned in the context of Figure 1. A side-fired unit, it contains a single row of 45 tubes, directly connected to the cold-shell outlet manifold. Present tube metallurgy is an HP-Nb micro-alloy (25Cr35NiNbTi). During investigation of a leak that transpired to be a manufacturing defect, evidence of metal dusting was observed in the static casting that formed the outlet of Tube 44. Figure 10 shows a macro-section of this static casting (left) welded to the centricast tube (right). Pitting is seen on both casting and tube and, more extensively, on the weld.

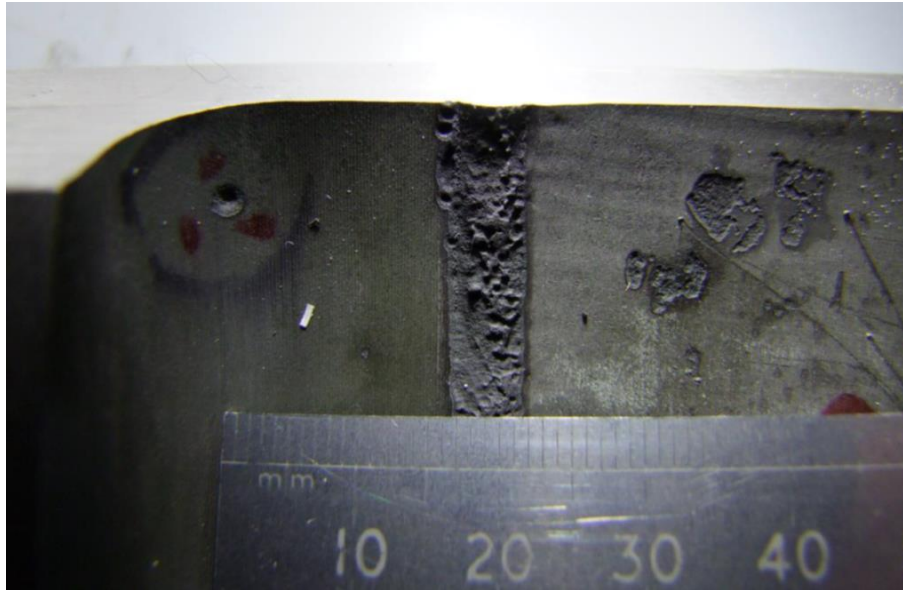
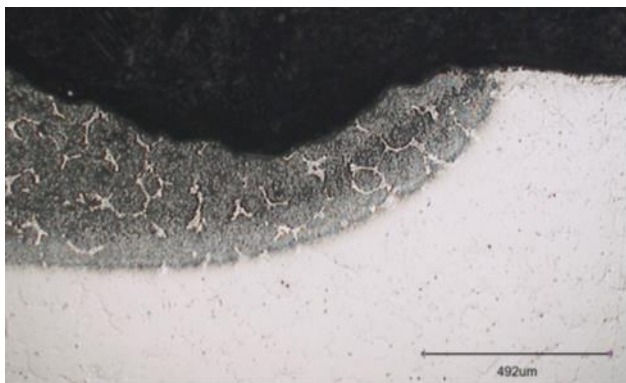
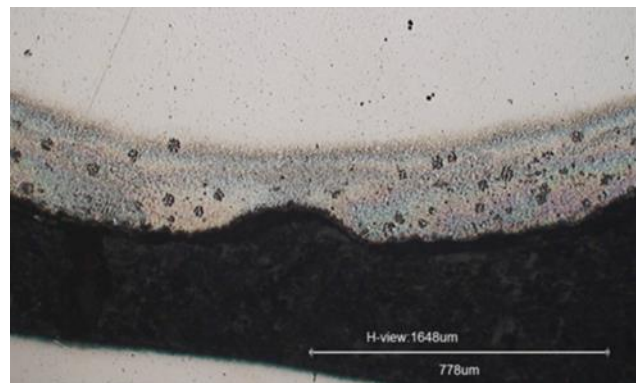


**Figure 10: Evidence of carburization and metal dusting in SMR Tube 44 outlet section**

Figure 11 shows metallographic sections of the pitted areas in the casting (left) and weld (right) of neighboring Tube 43; the field of view is approximately 1.5mm in each case. In both materials, a clear carburized zone is apparent surrounding the pits. The carburized zone in the weld metal contains numerous voids, evidence of the early stage of metal dusting.



(a) Outlet casting



(b) Weld metal

**Figure 11: Carburized zones surrounding the pits seen in neighboring Tube 43**

It is of interest to consider why this particular reformer has exhibited these phenomena. Figure 1 shows that carbon activity reaches unity at around 775°C for the Boudouard reaction under the stated outlet chemistry. Above this temperature, immunity from metal dusting is expected.

Figure 12 shows the thermal profile along the tube row, based on pyrometry measurements made over a six-month period. The maximum, mean and minimum temperatures are given for every tube that could be sighted. Vertical lines on the graph denote the burner positions – there are 6 rows of 9 burners on each side. The temperature distribution is most uneven, reflecting the irregular burner spacing, and shows distinct peaks and troughs. Regrettably, the same structural members of the firebox that force the irregular burner layout also preclude pyrometry of the tubes that are likely to be at the lowest temperatures.

Earlier in the unit's history several tubes were removed, and several others identified as critical, due to creep issues. Their locations are indicated on Figure 12 and it is seen that they are mostly associated with the higher temperature positions, as expected.

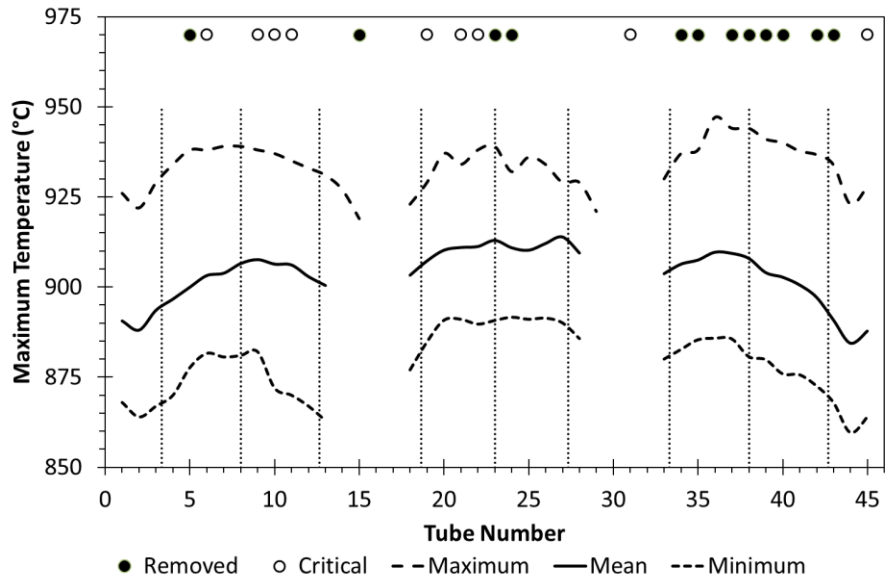


**Figure 12: Temperature variation along the SMR tube row – measured over 6 months**

By contrast, Tubes 43, 44 shown in Figures 10 and 11 are from the area where the lowest recorded temperatures occur. Given that the temperatures shown in Figure 12 come from within the firebox, but the tube outlets are located beneath the furnace floor and see no radiant heat, it is quite possible that the tube outlets come – at least intermittently – into the temperature range where metal dusting is possible. This would be rendered more likely if there is flow stagnation below the catalyst support basket which sits in the outlet casing or if there are any draughts below or through the furnace floor.

### CLOSURE

Carburization and metal dusting are phenomena of interesting chemistry and complicated metallurgy, particularly when interacting with other processes.

They are phenomena that impact on the structural integrity of affected components and therefore need to be understood in detail.

Detection and measurement of carburization and metal dusting are much facilitated by the availability of a validated non-destructive method.

Methods of remaining life prediction are available, which include all effects of carburization and metal dusting by logical extension of established procedures.

There are design factors and many process and operational factors that influence the susceptibility to and rate of progress of both phenomena. Careful consideration should always be given to the consequences of any changes made – not only in the unit where those changes are made but in those downstream of it.

## ACKNOWLEDGEMENTS

Thanks are due to many colleagues in refining and petrochemical plants for their contributions to the developments described here; discussions with engineers from many disciplines have been much appreciated. This paper is published with the permission of the Directors of R-TECH Consultants Ltd, John Brear – Plant Integrity, and Sonomatic Ltd – who jointly retain copyright.

## REFERENCES

1. H J Grabke, "Carburisation and Metal Dusting of Steels and High Temperature Alloys by Hydrocarbons", Chapter 1 of *Corrosion in Refineries*, J D Harston and F Ropital (Editors), European Federation of Corrosion Publication EFC 42, Cambridge, UK, Woodhead Publishing, 2007
2. H J Grabke, "Metal Dusting", Chapter 1 of *Corrosion by Carbon and Nitrogen: Metal Dusting, Carburisation and Nitridation*, H J Grabke and M Schütze (Editors), European Federation of Corrosion Publication EFC 41, Cambridge, UK, Woodhead Publishing, 2007
3. C M Chun and T A Ramanarayanan, "The Metal Dusting of Steels with Varying Concentrations of Chromium", Chapter 2 of *Corrosion by Carbon and Nitrogen: Metal Dusting, Carburisation and Nitridation*, H J Grabke and M Schütze (Editors), European Federation of Corrosion Publication EFC 41, Cambridge, UK, Woodhead Publishing, 2007
4. M Hansel, C A Boddington and D J Young "Internal Oxidation and Carburisation of Heat-Resistant Alloys", *Corrosion Science* 45 (2003) pp 967-981
5. J M Brear and J Williamson, "Integrity and Life Assessment of Catalytic Reformer Units", Chapter 2 of *Corrosion in Refineries*, J D Harston and F Ropital (Editors), European Federation of Corrosion Publication EFC 42, Cambridge, UK, Woodhead Publishing, 2007
6. J Cummings, J M Brear and A R Franks, "Failure of a 9Cr Platformer Heater Tube" NACE Technical Meeting, Houston, September 2007
7. J Harrison, J Cummings, M Carroll and J M Brear, "Carburisation and Metal Dusting of 9Cr Platformer Heater Tubes" NACE Technical Meeting, Houston, September 2007
8. API RP530, 7<sup>th</sup> Edition: "Calculation of Heater-tube Thickness in Petroleum Refineries", (Washington DC, USA, American Petroleum Institute), 2015
9. J M Brear, P Conlin, D Dechene, P Jarvis, and J Lilley, "Predicting and Preventing Carburisation-Induced Failures of Coker Heater Tubes" Coker.com Conf 'Delayed Coker Safety, Environment, Technology and Operations Optimization' Cologne, September 29 - October 2 2008